Neurobiological Changes Across Pregnancy: A Longitudinal Investigation

Yanbin Niu[1], Benjamin N. Conrad[1], M. Catalina Camacho[2], Sanjana Ravi[1], Hannah A. Piersiak[1], Lauren G. Bailes[1], Whitney Barnett[1], Mary Kate Manhard[3], David A. Cole[1], Ellen Wright Clayton[4,5], Sarah S. Osmundson[6], Seth A. Smith[7,8], Autumn Kujawa[1], and Kathryn L. Humphreys[1]

[1]Department of Psychology and Human Development, Peabody College, Vanderbilt University, Nashville, TN, USA

[2]Department of Psychiatry, Washington University in St. Louis, St. Louis, MO, USA

[3]Department of Radiology, Cincinnati Children's Hospital Medical Center, Cincinnati, OH, USA

[4]Center for Biomedical Ethics and Society, Department of Pediatrics, Vanderbilt University Medical Center, Nashville, TN, USA

[5]Law School, Vanderbilt University, Nashville, TN, USA

[6]Division of Maternal Fetal Medicine, Department of Obstetrics and Gynecology, Vanderbilt University Medical Center, Nashville, TN, USA

[7]Department of Radiology and Radiological Sciences, Vanderbilt University Institute of Imaging Science, Vanderbilt University Medical Center, Nashville, TN, USA

[8]Department of Biomedical Engineering, Vanderbilt University, Nashville, TN, USA

Abstract

Pregnancy is a period of profound biological transformation. However, we know remarkably little about pregnancy-related brain changes. To address this gap, we charted longitudinal changes in brain structure during pregnancy and explored potential mechanisms driving these changes. Ten participants (Mean age = 28.97 years) were assessed 1–6 times (median = 3) during their pregnancy. Each visit included anatomical and diffusion-weighted MRI, and assessments of waking salivary hormones, hair hormones, and inflammatory cytokines. Reductions in gray matter volume were found by gestational week. Neurite Density Index (NDI), a proxy of axon density, in white matter tracts increased across pregnancy, especially in tracts linked to sensorimotor processing. Progesterone levels were associated with reductions in brain volumetric measurements, and both progesterone and estradiol levels were linked to increases in NDI in white matter tracts. This study highlights the profound neurobiological changes experienced by pregnant individuals and provides insight on neuroplasticity in adulthood.

Keywords: pregnancy, neurobiological changes, hormones, gray matter, white matter

Introduction

Pregnancy is a period characterized by profound changes, including hormonal surges, increased blood volume, heightened oxygen consumption, as well as morphological adjustments like uterine expansion and relocation of organs[1–3]. These adaptations support fetal development and preparation for labor and delivery. The body's response to pregnancy may also change the pregnant person's brain, potentially as adaptive, nonadaptive, or merely evolutionary byproducts[4,5]. However, we know remarkably little about pregnancy-related brain changes. This knowledge gap regarding how, why, and to what extent the brain changes during pregnancy is, at least in part, attributable to historical reluctance in medical studies to include pregnant individuals due to concerns over potential risks and ethical complexities[6–9]. However, MRI has been used clinically among pregnant patients for the last four decades[10], and numerous studies find no evidence that MRI is associated with increased risk for adverse effects on pregnant individuals or their offspring (e.g., congenital anomalies, neoplasm, or vision or hearing loss)[11–13]. Given that approximately 85% of US women give birth in their lifetimes[14] and the existence of safe imaging procedures, it is critical that we now identify how a pregnant person's brain changes across pregnancy.

Non-human animal studies of pregnancy report diminished hippocampal cell proliferation[15,16] and a decline in microglial cell density[17], both of which may manifest as detectable reductions in gray matter volume. Additionally, evidence of brain volume reductions associated with pregnancy come from three human studies[18–21]. Notably, however, only four participants were assessed repeatedly during pregnancy in Oatridge et al.[20], and anatomical scans were collected via a 1.0-T MRI system, which has relatively low signal-to-noise ratio (SNR) and spatial resolution. Further, neither Hoekzema et al.[18,19], which compared women's brains before conception to 2-3 months postpartum, nor Paternina-Die et al.[21], both of whom conducted cross-sectional analyses between pregnant individuals and nulliparous controls, addressed changes occurring *within* pregnancy. Further, it is plausible that the physiological

changes occurring in pregnancy (e.g., novel sensory experiences and ongoing alterations in bodily functions, due to the growing uterus and the perception of fetal movements; Carlin & Alfirevic[22], might induce volumetric increases in brain regions related to sensorimotor processing and functioning. If so, this would be consistent with research on adult neuroplasticity emphasizing the brain's inherent capacity to restructure and adapt to varied environmental dynamics and experiences[23,24]. Moreover, although contemporary neuroscience acknowledges neuroplasticity in adults, structural changes that occur over the time scale of pregnancy (approximately 9 months) are typically quite subtle[25,26]. As such, it is plausible that the brain changes during pregnancy may be associated with gray matter decreases, increases, or little change.

In terms of potential pregnancy-related changes in white matter microstructure, non-human animal research observed an increase in myelinated axons during pregnancy, potentially resulting from augmented proliferation of oligodendrocytes—a type of brain cell vital for axonal myelination[27–29]. In particular, Chan et al.[30] reported a general increase in diffusivity across the whole brain during pregnancy, as well as regional increases in mean diffusivity (MD) and fractional anisotropy (FA) that were derived from Diffusion Tensor Imaging (DTI). In contrast, the only human study conducted by Hoekzema et al.[19] did not identify significant modifications in white matter diffusion metrics derived from DTI, nor did it detect changes in white matter volume in pregnant women as compared to nulliparous controls.

To better detect and understand the dynamics of brain changes during pregnancy, in vivo studies that document the brain structure longitudinally during pregnancy are crucial. Moreover, there are increasing calls for a more inclusive approach to biomedical research that recognizes and investigates the distinctive biological experiences of females[31–33]. Responding to this need, we initiated a pilot longitudinal study of pregnant people (n = 10, assessed 1–6 times [median = 3], spanning 12–39 gestational weeks). We utilized anatomical magnetic resonance imaging (MRI) to assess brain morphometry (e.g., gray matter volume and cortical thickness)

and multi-shell diffusion-weighted MRI with advanced modeling—neurite orientation dispersion and density (NODDI)[34]—to evaluate white matter microstructure. The primary goals of the current study were twofold. The first objective was to chart the brain structural changes occurring during pregnancy. The second goal was to explore potential mechanisms driving these changes, particularly focusing on pregnancy hormones, inflammatory cytokines, and total intracranial CSF volumes.

Methods

Participants. A total of 10 pregnant women aged between 20.00 and 39.25 years (*M* = 28.97, *SD* = 6.50) years were recruited for the current longitudinal study. In terms of race, 7 identified as White, 2 as Black or African American, and 1 selected "Other." In terms of ethnicity, 1 participant identified as Hispanic/Latine. Participants were recruited through online advertisements and referral/word of mouth and 1 participant was the senior author. Participant eligibility was initially screened via telephone. Inclusion criteria required participants to be pregnant, at least 18 years old, English-proficient, and have no immediate plans to relocate. Exclusion criteria encompassed a medical history of neurological injury or impairment, a history of psychosis, non-removable metal or electronic implants, having undergone in vitro fertilization (IVF), and use of medication(s) that could potentially influence hormonal or neurological changes during pregnancy (e.g., progesterone). The mean number of prior pregnancies carried to term was 0.50 (*SD* = 0.71, range = 0–2). The mean weeks gestation at data collection was 23.90 (*SD* = 7.70, range = 12.29–39.14). The number of data collection sessions for each participant ranged from 1 and 6 times (mean number of repeated measures = 2.70 times, *SD* = 1.49), contingent on individual circumstances and pregnancy progression. Fig. 1 provides a detailed illustration of the gestational timing range captured for each participant. Each session included an MRI scan and collection of hair samples and dried blood spots. Additionally, participants were asked to collect saliva samples at their homes on the morning prior to and the

morning of each session. All participants provided written informed consent prior to participation. Study procedures were approved by the Vanderbilt University Institutional Review Board.

Hormone Assessments. Hormonal assessments were performed by measuring levels of progesterone, estradiol, testosterone, and cortisol in saliva samples obtained from participants, in accordance with Salimetrics collection and assaying procedures. Two saliva samples were collected for each participant: one on the morning prior to the MRI scan and another on the day of the scan. The obtained values were then averaged for analysis. Additionally, we obtained estimates of cortisol, cortisone, and progesterone from hair samples. Further details on the saliva and hair sample collection and assay procedures can be found in the supplement. We primarily reported on salivary hormones, and results from hair hormone analysis were included in the supplement.

Inflammatory Cytokines Assessments. Inflammatory cytokine assessments were performed by measuring levels of Interleukin-6 (IL-6), Interleukin-10 (IL-10), Tumor Necrosis Factor alpha (TNFα), and C-Reactive Protein (CRP) in dried blood spots (DBS) obtained from participants. At each visit, up to 5 drops of capillary whole blood were collected on filter paper (Whatman 903) following a finger stick with a sterile microlancet. Blood was then dried at room temperature and stored at -20 degrees Celsius in accordance with protocols established by the Northwestern University's Laboratory for Human Biology Research[35,36], who performed assays on DBS samples. Further details on the DBS collection and assay procedures can be found in the supplement. The usability of the samples for IL-6, IL-10, and TNFα was constrained by the high volume requirements, resulting in a low yield of successfully assessed data for these cytokines (less than 50%). Thus, only CRP was utilized in the analyses. Detailed descriptive statistics are provided in Supplementary Table S1.

MRI Acquisition. MRI data acquisition was conducted on a 3T Philips Achieva scanner using a 32-channel head coil at Vanderbilt University Institute of Imaging Science. High-resolution T1- and T2-weighted images were obtained for each participant through 3D-quantification using an

interleaved Look–Locker acquisition sequence with a T2 preparation pulse (3D-QALAS) sequence[37] with the following parameters: repetition time (TR) of 5.0 ms, echo time (TE) of 2.3 ms, a flip angle of 4 degrees, a field of view (FOV) of 230 x 193 x 150 mm, a matrix size of 224 x 224 x 146, and a voxel size of 1 x 1 x 1 mm. The acquisition parameters of diffusion-weighted imaging (DWI) were as follows: TR of 4300 ms, TE of 91.5 ms, flip angle of 90 degrees, FOV of 240 x 240 x 135 mm, matrix size of 112 x 112 x 63, yielding a voxel size of 2 x 2 x 2 mm. The diffusion weighting was distributed across 23 directions with a b-value of 500 s/mm², 47 directions with a b-value of 1500 s/mm², and 70 directions with a b-value of 2500 s/mm². Further details about MRI acquisitions can be found in the supplement.

MRI Processing.

Anatomical MRI. Synthetic T1-weighted and T2-weighted images were found from 3D-QALAS images using SyntheticMR software (version 0.45.35; Linkoping, Sweden). Both T1-weighted and T2-weighted anatomical images were then used to extract structural MRI (sMRI) data through FreeSurfer v7.1.0's longitudinal pipeline[38]. Scans at every time point were independently processed for each participant (including skull stripping, Talairach transformation, subcortical structure labeling, surface extraction, spherical registration and cortical parcellation), followed by the creation of an unbiased within-subject template space using all the subject's time points[39]. Following the automated processing steps, all the cortical reconstructions were visually inspected for potential inaccuracies. We observed no processing failures and no manual edits were required. Subsequently, we obtained measurements of volume, surface area, and thickness morphometry for 68 cortical regions of interest from FreeSurfer's cortical parcellation (APARC) based on the Desikan-Killiany atlas[40].

CSF. To quantify the total CSF volume in the entire brain, we used the aggregated volume fraction of CSF image generated by SyntheticMR software from the 3D-QALAS images. Specifically, we first applied a threshold to retain voxels in which the CSF volume faction exceeded this threshold. Then, we multiplied the CSF volume fraction by the voxel volume

across the brain. For our primary analyses, we set a threshold at 80%, meaning that a voxel was classified as containing CSF if it has 80% or more CSF. To test if this threshold influenced findings, we repeated analyses using different thresholds across a range of 60% to 95% (reported in Table S4). We observed consistent results across these different probability thresholds.

Diffusion-weighted MRI. The raw diffusion data were processed using MRtrix3[41] and FMRIB's Software Library (FSL[42]). Preprocessing steps involved noise estimation and removal via the dwidenoise function from MRtrix3[43,44]. The eddy and susceptibility distortion corrections were performed using the dwifslpreproc function in MRtrix3[42,45–47]. Subsequent to preprocessing, we computed the neurite density index (NDI) and orientation dispersion index (ODI) using the NODDI Matlab Toolbox[34]. For comparison, we also fitted the standard DTI model[48]. In order to analyze changes across tracts, we first estimated fiber orientation distributions (FOD) using MRtrix3's dwi2fod msmt_csd and then normalized them using MRtrix3's mtnormalise[49,50]. The normalized FODs were then fed to TractSeg to automatically segment fiber tracts, resulting in NODDI and DTI metrics for each tract across 50 established tracts, which were subsequently used in our statistical analyses[51,52]. Lastly, we characterized the global changes for each NODDI metric and investigated if observed tract-level changes reflected a general alteration across all segmented tracts using two different approaches. For a more detailed description of diffusion data processing and metric quantification, please refer to the supplement.

Analytic Plan. Given the longitudinal nature of our data, analyses were conducted using linear mixed-effects (LME) models, utilizing the "lme4" package in R[53]. We organized analyses into two primary sections. First, we examined alterations in brain metrics throughout the course of pregnancy, where brain metrics ($BrainMetric_{ij}$) were the dependent variable and gestational week ($GesWeek_{ij}$) was the predictor. We also included age (Age_j) and total intracranial volume (TIV_j) as covariates for volumetric analyses (see Equation 1), and included Age_j and relative motion ($Motion_{ij}$) as covariates for diffusion metric analyses[54]; see Equation 2.

Equation 1:

Level 1: $BrainMetric_{ij} = \beta_{0j} + \beta_{1j}GesWeeks_{ij} + e_{ij}$ $\quad e_{ij} \sim N(0, \sigma_e^2)$

Level 2: $\beta_{0j} = \gamma_{00} + \gamma_{01}Age_j + \gamma_{02}TIV_j + u_{0j}$ $\quad u_{0j} \sim N(0, \tau_{00})$

$\beta_{1j} = \gamma_{10}$

Equation 2:

Level 1: $BrainMetric_{ij} = \beta_{0j} + \beta_{1j}GesWeeks_{ij} + \beta_{2j}Motion_{ij} + e_{ij}$ $\quad e_{ij} \sim N(0, \sigma_e^2)$

Level 2: $\beta_{0j} = \gamma_{00} + \gamma_{01}Age_j + u_{0j}$ $\quad u_{0j} \sim N(0, \tau_{00})$

$\beta_{1j} = \gamma_{10}$

$\beta_{2j} = \gamma_{20}$

where γ_{00} and u_{0j} are the fixed and random effects of the model intercept, and γ_{10} is the fixed effect of gestational weeks (i.e., slope).

The second set of analyses focused on the potential mechanisms underlying the observed brain alterations by examining the associations between brain metrics and potential influencing factors, including hormone levels, CRP, and CSF volume. We first applied LME models to examine variations in hormone levels (progesterone, estradiol, testosterone, and cortisol) and CRP throughout pregnancy, with hormone levels and CRP as the dependent variable and gestational week as the fixed effect. CRP was log-transformed using a base 10 logarithm to normalize their distribution[55]. For brain metrics demonstrating significant alterations during pregnancy, we examined potential links with hormone levels and the total intracranial CSF volume using LME models in which $BrainMetric_{ij}$ were the dependent variable and hormone levels ($Hormone_{ij}$) or CSF volume was the predictor. Given the absence of significant changes in CRP, associational analyses between CRP levels and observed changes in brain metrics were not implemented. Moreover, we included Age_j and total TIV_j as covariates for volumetric analyses (see Equation 3); we included Age_j and $Motion_{ij}$ as covariates for diffusion metric analyses (see Equation 4).

Equation 3:

Level 1: $BrainMetric_{ij} = \beta_{0j} + \beta_{1j}Hormone_{ij} + e_{ij}$ $\quad e_{ij} \sim N(0, \sigma_e^2)$

Level 2: $\beta_{0j} = \gamma_{00} + \gamma_{01}Age_j + \gamma_{02}TIV_j + u_{0j}$ $\quad u_{0j} \sim N(0, \tau_{00})$

$\beta_{1j} = \gamma_{10}$

Equation 4:

Level 1: $BrainMetric_{ij} = \beta_{0j} + \beta_{1j}Hormone_{ij} + \beta_{2j}Motion_{ij} + e_{ij}$ $\quad e_{ij} \sim N(0, \sigma_e^2)$

Level 2: $\beta_{0j} = \gamma_{00} + \gamma_{01}Age_j + u_{0j}$ $\quad u_{0j} \sim N(0, \tau_{00})$

$\beta_{1j} = \gamma_{10}$

$\beta_{2j} = \gamma_{20}$

where γ_{00} and u_{0j} are the fixed and random effects of the model intercept, and γ_{10} is the fixed effect of hormone slope.

Given the small sample size and the exploratory nature of our study, we did not correct for multiple comparisons[56]. Results with *p*-values < .05 were considered statistically significant. This decision was made to prioritize sensitivity over specificity, as it is particularly important in exploratory research to identify potential effects for further investigation in larger studies. Our results should therefore be interpreted with caution. We mitigated potential concerns by emphasizing our interpretation on the direction and magnitude of effect sizes. Additionally, recognizing the possibility that individual outliers could disproportionately influence the outcome in our small sample, we implemented leave-one-out analyses for our main findings, in which each participant was systematically removed and the analyses recomputed. This approach helps to validate that the observed effects are consistent and not artifacts of unique data points, thus enhancing the reliability of our findings[57]. We also considered the patterns of results across related dependent measures, as opposed to individual tests in isolation. The results of our study thus serve as a preliminary exploration into the complex domain of neurobiological dynamics during pregnancy.

Results

Brain Changes during Pregnancy

Brain Morphometry Changes. Covarying for TIV and age, the total brain volume exhibited decreases across pregnancy (β = -0.105, 95% CI [-0.169, -0.040], p = .004). This translates to a 2.6% decline over the observed gestational range in this study (i.e., 12–39 weeks). We further conducted leave-one-out analyses, which resulted in estimated β values that ranged from -0.184 to -0.090. Similarly, total gray matter volume exhibited decreases across pregnancy (β = -0.192, 95% CI [-0.301, -0.082], p = .002). This translates to a 3.9% decline over the observed gestational range in this study (see Fig. 2). With leave-one-out analyses, β values ranged from -0.328 to -0.179. There were decreases in total cortical volume (β = -0.238, 95% CI [-0.374, -0.102], p = .002) and in subcortical volume (β = -0.094, 95% CI [-0.196, 0.008], p = .068), although the latter was not statistically significant. Additionally, there were large decreases in cortical thickness (β = -0.516, 95% CI [-0.915, -0.116], p = .015), yet cortical surface area remained unchanged (β = -0.018, 95% CI [-0.052, 0.017], p = .297). These results suggest that the observed reduction in total gray matter volume may primarily result from decreases in cortical volume, and more specifically, decreases in cortical thickness (see Fig. S1 for detailed statistics). Lastly, total white matter volume did not exhibit a statistically significant change across pregnancy (β = -0.031, 95% CI [-0.120, 0.057], p = .460). All findings were consistent using leave-one-out analyses, as detailed in Table S2.

Changes in Cortical Regions. To further characterize the reduction in total cortical volume, we fitted LME models for all Desikan-Killiany atlas regions, using gestational week as the fixed effect and hemisphere, TIV, and age as covariates. A surface map with the standardized regression coefficients for all cortex regions are shown in Fig. 3A. Overall, we observed a consistent trend of decreasing cortical volume in most cortical regions, except for three regions in the occipital lobe (pericalcarine, lingual, and cuneus) and two regions in the medial temporal

lobe (entorhinal and temporal pole). Statistically significant reductions in cortical volumes were observed in prefrontal cortex regions, including the medial orbitofrontal, superior frontal, and lateral orbitofrontal cortex, as well as two regions surrounding the central sulcus: the precentral and postcentral cortex (Fig. 3B). Detailed statistical reports are provided in Table S3.

White Matter Microstructure Changes. In our investigation of changes in white matter microstructure, we implemented LME models for each of the NODDI metrics (NDI and ODI) across each of the 50 tracts generated by TractSeg with gestational week as the fixed effect, and hemisphere (where applicable), age, and relative motion as covariates. To facilitate the understanding of the global pattern of metric changes, a heat map was generated, representing the standardized regression coefficients for all segmented tracts (see Fig. S2). Throughout the gestation period, we observed a predominant increase in NDI across most tracts, whereas ODI metrics remained relatively stable. Notably, the most pronounced increases in NDI were observed in projection tracts such as the corticospinal tract (CST), fronto-pontine tract (FPT), parieto-occipital pontine (PORT), in addition to the striato-premotor tract (ST_PREM) and arcuate fascicle (AF) (see Fig. 4). In line with these NDI findings, our analysis of DTI metrics revealed a predominant trend of increasing FA. Tracts that exhibited the most significant FA increases largely overlapped with those displaying notable NDI increases. Comprehensive statistical results for NDI and ODI metrics are available in Tables S6 and S7, and analyses of DTI metrics can also be found in the supplement. Lastly, an examination of average measures across all segmented tracts revealed no significant global changes in NDI and ODI metrics during pregnancy, consistent with our secondary method for assessing global diffusion metrics (see supplement).

CSF Changes. We found a statistically significant increase in total intracranial CSF (β = 0.187, 95% CI [0.021, 0.353], p = .030) after covarying for age and TIV (see Fig. 5). Using a leave-one-out cross-validation approach, the β values ranged from 0.145 to 0.267 (see Table S4). This

pattern was consistent when varying the threshold of CSF volume fraction between 60% and 95% (Table S5).

Associations Between Brain Dynamics and Salivary Hormones in Pregnancy

Salivary Hormones and Inflammatory Cytokines Changes during Pregnancy. Covarying for age, we observed statistically significant increases in waking salivary levels of progesterone (β = 0.717, 95% CI [0.391, 1.042], p < .001), estradiol (β = 0.792, 95% CI [0.533, 1.050], p < .001), and testosterone (β = 0.393, 95% CI [0.061, 0.724], p = .024) across pregnancy. The increase in cortisol levels was not statistically significant (β = 0.198, 95% CI [-0.014, 0.410], p = .065). Additionally, we did not observe statistically significant changes in CRP levels throughout the course of pregnancy (β = -0.067, 95% CI [-0.248, 0.114], p = .441; see Fig. S5).

Associations Between Salivary Hormones and Brain Structure. After covarying for TIV and age, we found statistically significant negative associations between total brain volume and salivary levels of progesterone (β = -0.103, 95% CI [-0.170, -0.036], p = .006) and cortisol (β = -0.213, 95% CI [-0.393, -0.032], p = .025), indicating that increasing salivary levels of progesterone and cortisol are associated with decreasing total brain volume. Associations between total brain volume and either salivary estradiol or testosterone levels were not statistically significant (ps > .144). Additionally, total gray matter volume was negatively associated with salivary progesterone (β = -0.189, 95% CI [-0.305, -0.073], p = .003), but not salivary estradiol, testosterone, or cortisol (all ps > .134). Total cortical volume (β = -0.254, 95% CI [-0.390, -0.118], p = .002) and mean cortical thickness (β = -0.691, 95% CI [-1.049, 0.333], p = .001) were also negatively associated with salivary progesterone (see Fig. 6), but not with salivary estradiol, testosterone, and cortisol levels (all ps > .137).

Associations Between Salivary Hormones and Diffusion Metrics. Fig. S7 show the standardized regression coefficients of hormone levels across all segmented tracts, illustrating the association between NDI and salivary hormone levels. Most notably, our results indicated

that NDI across nearly all tracts was positively associated with salivary estradiol levels and moderately with salivary progesterone (see Fig. 7). Moreover, NDI demonstrated a negative link with salivary cortisol levels, while no association was found with salivary testosterone. Detailed statistical outcomes of these analyses are available in Table S12-S15.

Associations Between Salivary Hormones and CSF. Covarying for TIV and age, no statistically significant association was detected between volume changes and salivary hormonal levels, including progesterone (β = 0.130, 95% CI [-0.060, 0.319], p = .160), estradiol (β = 0.151, 95% CI [-0.060, 0.361], p = .143), testosterone (β = 0.153, 95% CI [-0.119, 0.425], p = .242), and cortisol (β = 0.187, 95% CI [-0.284, 0.668], p = .401; see Table S16-S19).

Associations Between CSF and Brain Structure. There were statistically significant negative associations between total intracranial CSF and total brain volume (β = -0.277, 95% CI [-0.452, -0.102], p = .004), total gray matter volume (β = -0.388, 95% CI [-0.678, -0.097], p = .013), and total cortical volume (β = -0.391, 95% CI [-0.754, -0.028], p = .037), suggesting that reduction in brain volumetrics is associated with the increase in the total intracranial CSF volume. The link between total intracranial CSF and mean cortical thickness was not statistically significant (β = -0.515, 95% CI [-1.069, 0.039], p = .066).

Associations Between CSF and Diffusion Metrics. Across all segmented tracts, there were no statistically significant associations between total intracranial CSF and NDI. Detailed statistical outcomes of these analyses are available in Table S20.

Discussion

In a sample of 10 pregnant participants who underwent multimodal MRI scans, hormone assessments, and inflammatory cytokine assessments between 1 and 6 times during pregnancy (median = 3 times), we explored whether, and to what degree, neurobiological changes occur during pregnancy. There were four main findings. First, there were pronounced reductions in overall brain and gray matter volume, while an increase was found in the total intracranial CSF

volume. Second, using NODDI metrics to assess white matter microstructure, we found an increase in NDI across the majority of segmented tracts, with the most pronounced increase observed in tracts associated with sensorimotor processing. Third, there was a significant correlation between pregnancy-related salivary hormones and observed brain changes (i.e., volumetric reduction in overall brain and gray matter, and increased NDI in segmented tracts). Fourth, the increase in the total intracranial CSF volume was associated with the decrease in brain volumetrics, but not with NDI changes.

The decreases in estimates of total brain volume in the present study were consistent with earlier evidence involving both humans[18–21,58] and non-human animal models[15–17]. Comparing mothers before and after their first pregnancy, Hoekzema et al.[18,19] observed a reduction in gray matter volume across multiple brain regions, notably within the anterior and posterior midline structures. Another recent study found that, during late pregnancy, mothers exhibited smaller global cortical volume and thickness compared to nulliparous controls, with the most pronounced differences in the somatomotor, attentional, and default mode networks[21]. A recent preprint by Pritschet et al.[58] focused on neuroanatomical changes from preconception to two years postpartum in an individual, documenting significant reductions in gray matter volume and cortical thickness. Non-human animal studies suggest that the observed brain volume reduction may be linked to reduced microglial proliferation, as evidenced by the reduced microglial cell density in pregnant rats during late gestation and the early postpartum period compared to virgin rats[17]. Expanding upon previous pre- and post-pregnancy comparisons and cross-sectional analyses, our findings demonstrate a significant rate of reduction in gray matter volume during pregnancy. Additionally, we found a significant correlation between CSF volume and overall brain and gray matter volumes. This association suggests that intracranial CSF volume increases during pregnancy, consistent with the prior report of ventricular volume expansion[20], may result in pressure on the brain and compression of the cortex, possibly contributing to the observed decrease in brain volume[59,60].

Additionally, we observed an increase in NDI across tracts, especially those linked with sensorimotor processing, whereas the ODI remained largely unchanged. NDI quantifies the tissue volume fraction occupied by neurites, such as axons and dendrites, and is considered as a proxy for axonal density in white matter[61,62]. Meanwhile, ODI reflects the variance in neurite orientation. Our findings suggest that across pregnancy there may be an increase in axonal density, potentially stemming from increased myelination and/or axonal diameter, without significant shifts in white matter geometric complexity. This aligns with prior non-human animal studies that have documented an increase in myelinated axons during pregnancy, potentially as a result of amplified proliferation of oligodendrocytes[27–29]. However, there is a discrepancy between our results and those reported by Hoekzema et al.[19] who did not observe significant changes in DTI metrics during pregnancy. The discrepancy may arise from variations in imaging sequence parameters. For instance, Hoekzema et al.[19] used single shell protocol (b = 1000) in contrast to the multi-shell protocol (b = 500, 1500, 2500) in the present study, which has been shown to affect the estimated scalar diffusion metrics[63]. Another consideration is the methodological divergence between the two studies. Our study adopted a longitudinal design, capturing dynamic changes over the course of pregnancy, while Hoekzema et al.[19] employed a pre-post pregnancy comparison approach. Their post-pregnancy data acquisition took place, on average, 100 days after childbirth coupled with a wide variability (*SD* = 70 days). This extended interval could potentially obscure white matter alterations occurring during pregnancy. Indeed, the recent preprint by Pritschet et al.[58] demonstrated an increase in global quantitative anisotropy (QA), an index of white matter microstructural integrity, during gestation, which was concomitant with rises in estradiol and progesterone. However, extended analyses into the postpartum period revealed non-linear patterns of global QA, with increases observed throughout the first and second trimesters, returning to baseline levels postpartum. Thus, it is possible that white matter quickly reverts to its pre-pregnancy state, thereby remaining undetected in the delayed post-pregnancy assessment. Alternatively, the postpartum period

itself, characterized by hormonal fluctuations, physiological adaptations, and new caregiving demands, might induce its own set of white matter microstructural adaptations, which might counteract those taking place during pregnancy.

The current study also explored candidate mechanisms underlying the observed neurobiological changes during pregnancy. First, our data revealed a correlation between pregnancy-associated hormones and brain alterations in both gray matter and white matter. Estradiol and progesterone are pivotal neuroprotective agents, modulating processes like neurogenesis[64,65], dendritic spine and branching[66,67], myelination[68,69], axonal growth, and synaptogenesis[70]. Our findings of positive correlations between white matter NDI with progesterone and estradiol levels, are consistent with such findings from animal studies. However, the observed inverse associations between pregnancy-related hormones and gray matter volumes is somewhat counterintuitive, especially when considering that non-human animal research suggests estradiol and progesterone promote neurogenesis[71,72]. It might be that increased dendritic length and branching, spine density in gray matter due to pregnancy-related hormones[66,66,67,70,73] and/or myelination lead to misclassification of voxels at tissue interfaces, thereby appearing as reductions in gray matter volume[74,75], either in addition to or instead of fluid-related compression. It is also possible that hormones influence other physiological functions that are linked to a decrease in gray matter volume. For example, suppressed microglial proliferation might underlie the connections between hormonal shifts and grey matter reduction during pregnancy[75]. Moreover, the influence of pregnancy-related hormones likely represents only one of factors contributing to observed brain changes. Other reproductive-associated alterations, such as augmented water content[76,77] and blood flow variations[78,79] during pregnancy, may also play significant roles. For example, studies have documented a significant and progressive rise in total body water, extracellular, and intracellular water values throughout pregnancy[76,77], which might explain the observed elevation in NDI. Yet, it is important to note that in vivo MRI methods offer insights at a macroscopic level and

inherently lack the resolution to elucidate the cellular and molecular mechanisms at play during pregnancy. Future research at different levels is needed to supplement this work and enhance our understanding of the neurobiological changes observed during pregnancy.

Several limitations merit consideration. Our study was constrained by a small sample size and a limited number of observations (27 unique scan sessions from 10 individuals), with some participants attending only a single session. Power to detect subtle effects is therefore limited as well as our ability to adjust for potential confounds. Moreover, our sample did not cover the entire duration of pregnancy. Without preconception data we have an incomplete picture of when during pregnancy such alterations become evident. Additionally, given the preliminary nature of our investigation, we opted not to implement corrections for multiple comparisons. Although this decision enhances our sensitivity to potential effects, it simultaneously raises the risk of type I errors. However, the consistency in patterns and lack of randomness suggest that the results may not be artifacts but are likely indicative of genuine underlying phenomena. It is important for subsequent, larger-scale studies to incorporate appropriate corrections to further validate and replicate our observations. Furthermore, our exploration of the underlying mechanisms of neural dynamics primarily focused on hormonal fluctuations during pregnancy. Although these hormonal shifts are important, they might represent just one aspect of a more multifaceted interplay. Other potential factors, such as immune system modulations, metabolic changes, vascular dynamics, and alterations in neurotransmitter levels, may also significantly contribute. Future research with an interdisciplinary approach, integrating insights from these domains would shed light on the multifaceted nature of brain changes during pregnancy.

The present study elucidates neurobiological changes occurring across pregnancy. Specifically, we observed a decline in total brain and gray matter volume, predominantly within midline cortical regions. Total intracranial CSF volume significantly increased. Furthermore, the NDI in white matter tracts increased across pregnancy, particularly in tracts related to

sensorimotor processing. Our data also suggests that increases in CSF and pregnancy-related hormones may, at least partially, contribute to these observed neural alterations. These findings highlight neuroplasticity during pregnancy, establishing a foundation for further investigations in this essential, yet understudied area of research.

ACKNOWLEDGMENTS. We extend our sincere gratitude to all participants for their contributions to this study. This research was supported by the Peabody Small Grant, Vanderbilt Brain Institute Trans-Institutional Program (TIPs) Grant, and Vanderbilt Institute for Clinical and Translational Research Grant (VR61621) to KLH. Author contributions were supported in part by T32MH18921 (HAP; LGB).

References

1. Kazma, J. M., van den Anker, J., Allegaert, K., Dallmann, A. & Ahmadzia, H. K. Anatomical and physiological alterations of pregnancy. *J. Pharmacokinet. Pharmacodyn.* **47**, 271–285 (2020).
2. Soma, -Pillay Priya, Nelson, -Piercy Catherine, Tolppanen, H. & Mebazaa, A. Physiological changes in pregnancy : review articles. *Cardiovasc. J. Afr.* **27**, 89–94 (2016).
3. Tan, E. K. & Tan, E. L. Alterations in physiology and anatomy during pregnancy. *Best Pract. Res. Clin. Obstet. Gynaecol.* **27**, 791–802 (2013).
4. Cárdenas, E. F., Kujawa, A. & Humphreys, K. L. Neurobiological changes during the peripartum period: implications for health and behavior. *Soc. Cogn. Affect. Neurosci.* **15**, 1097–1110 (2020).
5. Martínez-García, M., Cardenas, S. I., Pawluski, J., Carmona, S. & Saxbe, D. E. Recent Neuroscience Advances in Human Parenting. in *Patterns of Parental Behavior: From Animal Science to Comparative Ethology and Neuroscience* (ed. González-Mariscal, G.) 239–267 (Springer International Publishing, Cham, 2022). doi:10.1007/978-3-030-97762-7_8.
6. Chartier, A. L. *et al.* The Safety of Maternal and Fetal MRI at 3 T. *Am. J. Roentgenol.* **213**, 1170–1173 (2019).
7. *Women and Health Research: Ethical and Legal Issues of Including Women in Clinical Studies*. (National Academies Press (US), Washington (DC), 1999).
8. Merkatz, R. B. Inclusion of Women in Clinical Trials: A Historical Overview of Scientific, Ethical, and Legal Issues. *J. Obstet. Gynecol. Neonatal Nurs.* **27**, 78–84 (1998).
9. Weld, E. D., Bailey, T. C. & Waitt, C. Ethical issues in therapeutic use and research in pregnant and breastfeeding women. *Br. J. Clin. Pharmacol.* **88**, 7–21 (2022).
10. Lowe, T. W., Weinreb, J., Santos-Ramos, R. & Cunningham, F. G. Magnetic Resonance Imaging in Human Pregnancy. *Obstet. Gynecol.* **66**, 629 (1985).

11. Choi, J. S. *et al.* A case series of 15 women inadvertently exposed to magnetic resonance imaging in the first trimester of pregnancy. *J. Obstet. Gynaecol.* **35**, 871–872 (2015).
12. Ray, J. G., Vermeulen, M. J., Bharatha, A., Montanera, W. J. & Park, A. L. Association Between MRI Exposure During Pregnancy and Fetal and Childhood Outcomes. *JAMA* **316**, 952–961 (2016).
13. Tee, L. M., Kan, E. Y., Cheung, J. C. & Leung, W. Magnetic resonance imaging of the fetal brain. *Hong Kong Med. J.* **22**, 270 (2016).
14. U.S. Census Bureau. Fertility of women in the United States. *Current Population Reports: US Census Bureau* https://www.census.gov/data/tables/2018/demo/fertility/women-fertility.html (2018).
15. Eid, R. S. *et al.* Early and late effects of maternal experience on hippocampal neurogenesis, microglia, and the circulating cytokine milieu. *Neurobiol. Aging* **78**, 1–17 (2019).
16. Pawluski, J. L. *et al.* Effect of sertraline on central serotonin and hippocampal plasticity in pregnant and non-pregnant rats. *Neuropharmacology* **166**, 107950 (2020).
17. Haim, A. *et al.* A survey of neuroimmune changes in pregnant and postpartum female rats. *Brain. Behav. Immun.* **59**, 67–78 (2017).
18. Hoekzema, E. *et al.* Pregnancy leads to long-lasting changes in human brain structure. *Nat. Neurosci.* **20**, 287–296 (2017).
19. Hoekzema, E. *et al.* Mapping the effects of pregnancy on resting state brain activity, white matter microstructure, neural metabolite concentrations and grey matter architecture. *Nat. Commun.* **13**, 6931 (2022).
20. Oatridge, A. *et al.* Change in Brain Size during and after Pregnancy: Study in Healthy Women and Women with Preeclampsia. *Am. J. Neuroradiol.* **23**, 19–26 (2002).
21. Paternina-Die, M. *et al.* Women's neuroplasticity during gestation, childbirth, and postpartum. https://www.researchsquare.com (2023) doi:10.21203/rs.3.rs-2723150/v1.

22. Carlin, A. & Alfirevic, Z. Physiological changes of pregnancy and monitoring. *Best Pract. Res. Clin. Obstet. Gynaecol.* **22**, 801–823 (2008).

23. Maguire, E. A. *et al.* Navigation-related structural change in the hippocampi of taxi drivers. *Proc. Natl. Acad. Sci.* **97**, 4398–4403 (2000).

24. May, A. Experience-dependent structural plasticity in the adult human brain. *Trends Cogn. Sci.* **15**, 475–482 (2011).

25. Bethlehem, R. a. I. *et al.* Brain charts for the human lifespan. *Nature* **604**, 525–533 (2022).

26. Walhovd, K. B. *et al.* Consistent neuroanatomical age-related volume differences across multiple samples. *Neurobiol. Aging* **32**, 916–932 (2011).

27. Gregg, C. Pregnancy, prolactin and white matter regeneration. *J. Neurol. Sci.* **285**, 22–27 (2009).

28. Gregg, C. *et al.* White Matter Plasticity and Enhanced Remyelination in the Maternal CNS. *J. Neurosci.* **27**, 1812–1823 (2007).

29. Kalakh, S. & Mouihate, A. Enhanced remyelination during late pregnancy: involvement of the GABAergic system. *Sci. Rep.* **9**, 7728 (2019).

30. Chan, R. W. *et al.* Structural and Functional Brain Remodeling during Pregnancy with Diffusion Tensor MRI and Resting-State Functional MRI. *PLOS ONE* **10**, e0144328 (2015).

31. Beery, A. K. & Zucker, I. Sex bias in neuroscience and biomedical research. *Neurosci. Biobehav. Rev.* **35**, 565–572 (2011).

32. Clayton, J. A. & Collins, F. S. Policy: NIH to balance sex in cell and animal studies. *Nature* **509**, 282–283 (2014).

33. Ferretti, M. T., Women's Brain Project & Galea, L. A. M. Improving pharmacological treatment in brain and mental health disorders: the need for gender and sex analyses. *Front. Neuroendocrinol.* **50**, 1–2 (2018).

34. Zhang, H., Schneider, T., Wheeler-Kingshott, C. A. & Alexander, D. C. NODDI: Practical in vivo neurite orientation dispersion and density imaging of the human brain. *NeuroImage* **61**, 1000–1016 (2012).

35. McDade, T. W. Development and validation of assay protocols for use with dried blood spot samples. *Am. J. Hum. Biol.* **26**, 1–9 (2014).

36. Miller, E. M. & Mcdade, T. W. A highly sensitive immunoassay for interleukin-6 in dried blood spots. *Am. J. Hum. Biol.* **24**, 863–865 (2012).

37. Fujita, S. *et al.* 3D quantitative synthetic MRI-derived cortical thickness and subcortical brain volumes: Scan–rescan repeatability and comparison with conventional T1-weighted images. *J. Magn. Reson. Imaging* **50**, 1834–1842 (2019).

38. Fischl, B. FreeSurfer. *NeuroImage* **62**, 774–781 (2012).

39. Reuter, M., Schmansky, N. J., Rosas, H. D. & Fischl, B. Within-subject template estimation for unbiased longitudinal image analysis. *NeuroImage* **61**, 1402–1418 (2012).

40. Desikan, R. S. *et al.* An automated labeling system for subdividing the human cerebral cortex on MRI scans into gyral based regions of interest. *NeuroImage* **31**, 968–980 (2006).

41. Tournier, J.-D. *et al.* MRtrix3: A fast, flexible and open software framework for medical image processing and visualisation. *NeuroImage* **202**, 116137 (2019).

42. Smith, S. M. *et al.* Advances in functional and structural MR image analysis and implementation as FSL. *NeuroImage* **23**, S208–S219 (2004).

43. Veraart, J., Fieremans, E. & Novikov, D. S. Diffusion MRI noise mapping using random matrix theory. *Magn. Reson. Med.* **76**, 1582–1593 (2016).

44. Veraart, J. *et al.* Denoising of diffusion MRI using random matrix theory. *NeuroImage* **142**, 394–406 (2016).

45. Andersson, J. L. R. & Sotiropoulos, S. N. An integrated approach to correction for off-resonance effects and subject movement in diffusion MR imaging. *NeuroImage* **125**, 1063–1078 (2016).

46. Andersson, J. L. R., Graham, M. S., Zsoldos, E. & Sotiropoulos, S. N. Incorporating outlier detection and replacement into a non-parametric framework for movement and distortion correction of diffusion MR images. *NeuroImage* **141**, 556–572 (2016).

47. Bastiani, M. *et al.* Automated quality control for within and between studies diffusion MRI data using a non-parametric framework for movement and distortion correction. *NeuroImage* **184**, 801–812 (2019).

48. Basser, P. J., Mattiello, J. & LeBihan, D. MR diffusion tensor spectroscopy and imaging. *Biophys. J.* **66**, 259–267 (1994).

49. Jeurissen, B., Tournier, J.-D., Dhollander, T., Connelly, A. & Sijbers, J. Multi-tissue constrained spherical deconvolution for improved analysis of multi-shell diffusion MRI data. *NeuroImage* **103**, 411–426 (2014).

50. Tournier, J.-D., Calamante, F., Gadian, D. G. & Connelly, A. Direct estimation of the fiber orientation density function from diffusion-weighted MRI data using spherical deconvolution. *NeuroImage* **23**, 1176–1185 (2004).

51. Wasserthal, J. *et al.* Multiparametric mapping of white matter microstructure in catatonia. *Neuropsychopharmacology* **45**, 1750–1757 (2020).

52. Wasserthal, J., Neher, P. & Maier-Hein, K. H. TractSeg - Fast and accurate white matter tract segmentation. *NeuroImage* **183**, 239–253 (2018).

53. Bates, D., Mächler, M., Bolker, B. & Walker, S. Fitting Linear Mixed-Effects Models Using lme4. *J. Stat. Softw.* **67**, (2015).

54. Yendiki, A., Koldewyn, K., Kakunoori, S., Kanwisher, N. & Fischl, B. Spurious group differences due to head motion in a diffusion MRI study. *NeuroImage* **88**, 79–90 (2014).

55. Ragsdale, H. B., Kuzawa, C. W., Borja, J. B., Avila, J. L. & McDade, T. W. Regulation of inflammation during gestation and birth outcomes: Inflammatory cytokine balance predicts birth weight and length. *Am. J. Hum. Biol. Off. J. Hum. Biol. Counc.* **31**, e23245 (2019).

56. Althouse, A. D. Adjust for Multiple Comparisons? It's Not That Simple. *Ann. Thorac. Surg.* **101**, 1644–1645 (2016).

57. Hastie, T., Tibshirani, R., Friedman, J. H. & Friedman, J. H. *The Elements of Statistical Learning: Data Mining, Inference, and Prediction*. vol. 2 (Springer, 2009).

58. Pritschet, L. *et al.* Neuroanatomical changes observed over the course of a human pregnancy. 2023.12.14.571688 Preprint at https://doi.org/10.1101/2023.12.14.571688 (2023).

59. Kang, K., Kwak, K., Yoon, U. & Lee, J.-M. Lateral Ventricle Enlargement and Cortical Thinning in Idiopathic Normal-pressure Hydrocephalus Patients. *Sci. Rep.* **8**, 13306 (2018).

60. Sakka, L., Coll, G. & Chazal, J. Anatomy and physiology of cerebrospinal fluid. *Eur. Ann. Otorhinolaryngol. Head Neck Dis.* **128**, 309–316 (2011).

61. Jespersen, S. N. *et al.* Neurite density from magnetic resonance diffusion measurements at ultrahigh field: Comparison with light microscopy and electron microscopy. *NeuroImage* **49**, 205–216 (2010).

62. Sepehrband, F. *et al.* Brain tissue compartment density estimated using diffusion‐weighted MRI yields tissue parameters consistent with histology. *Hum. Brain Mapp.* **36**, 3687–3702 (2015).

63. Correia, M. M., Carpenter, T. A. & Williams, G. B. Looking for the optimal DTI acquisition scheme given a maximum scan time: are more b-values a waste of time? *Magn. Reson. Imaging* **27**, 163–175 (2009).

64. Azcoitia, I., Barreto, G. E. & Garcia-Segura, L. M. Molecular mechanisms and cellular events involved in the neuroprotective actions of estradiol. Analysis of sex differences. *Front. Neuroendocrinol.* **55**, 100787 (2019).

65. Montes, P. *et al.* Progesterone treatment in rats after severe global cerebral ischemia promotes hippocampal dentate gyrus neurogenesis and functional recovery. *Neurol. Res.* **41**, 429–436 (2019).

66. Cooke, B. M. & Woolley, C. S. Gonadal hormone modulation of dendrites in the mammalian CNS. *J. Neurobiol.* **64**, 34–46 (2005).

67. Sanchez, A. M., Flamini, M. I., Genazzani, A. R. & Simoncini, T. Effects of Progesterone and Medroxyprogesterone on Actin Remodeling and Neuronal Spine Formation. *Mol. Endocrinol.* **27**, 693–702 (2013).

68. Ibanez, C. *et al.* Systemic progesterone administration results in a partial reversal of the age-associated decline in CNS remyelination following toxin-induced demyelination in male rats. *Neuropathol. Appl. Neurobiol.* **30**, 80–89 (2004).

69. Ibanez, C. *et al.* Steroids and the reversal of age-associated changes in myelination and remyelination. *Prog. Neurobiol.* **71**, 49–56 (2003).

70. Haraguchi, S. *et al.* Estradiol Promotes Purkinje Dendritic Growth, Spinogenesis, and Synaptogenesis During Neonatal Life by Inducing the Expression of BDNF. *The Cerebellum* **11**, 416–417 (2012).

71. Arevalo, M. A. *et al.* Molecular mechanisms involved in the regulation of neuritogenesis by estradiol: Recent advances. *J. Steroid Biochem. Mol. Biol.* **131**, 52–56 (2012).

72. Chen, S., Kumar, N., Mao, Z., Sitruk-Ware, R. & Brinton, R. D. Therapeutic progestin segesterone acetate promotes neurogenesis: implications for sustaining regeneration in female brain. *Menopause* **25**, 1138 (2018).

73. Keyser-Marcus, L. *et al.* Alterations of medial preoptic area neurons following pregnancy and pregnancy-like steroidal treatment in the rat. *Brain Res. Bull.* **55**, 737–745 (2001).

74. Natu, V. S. *et al.* Apparent thinning of human visual cortex during childhood is associated with myelination. *Proc. Natl. Acad. Sci.* **116**, 20750–20759 (2019).

75. Servin-Barthet, C. *et al.* The transition to motherhood: linking hormones, brain and behaviour. *Nat. Rev. Neurosci.* **24**, 605–619 (2023).

76. Valensise, H. *et al.* Multifrequency bioelectrical impedance analysis in women with a normal and hypertensive pregnancy12. *Am. J. Clin. Nutr.* **72**, 780–783 (2000).

77. Van Loan, M. D., Kopp, L. E., King, J. C., Wong, W. W. & Mayclin, P. L. Fluid changes during pregnancy: use of bioimpedance spectroscopy. *J. Appl. Physiol.* **78**, 1037–1042 (1995).

78. Nevo, O., Soustiel, J. F. & Thaler, I. Maternal cerebral blood flow during normal pregnancy: a cross-sectional study. *Am. J. Obstet. Gynecol.* **203**, 475.e1-475.e6 (2010).

79. Osol, G., Ko, N. L. & Mandalà, M. Plasticity of the Maternal Vasculature During Pregnancy. *Annu. Rev. Physiol.* **81**, 89–111 (2019).

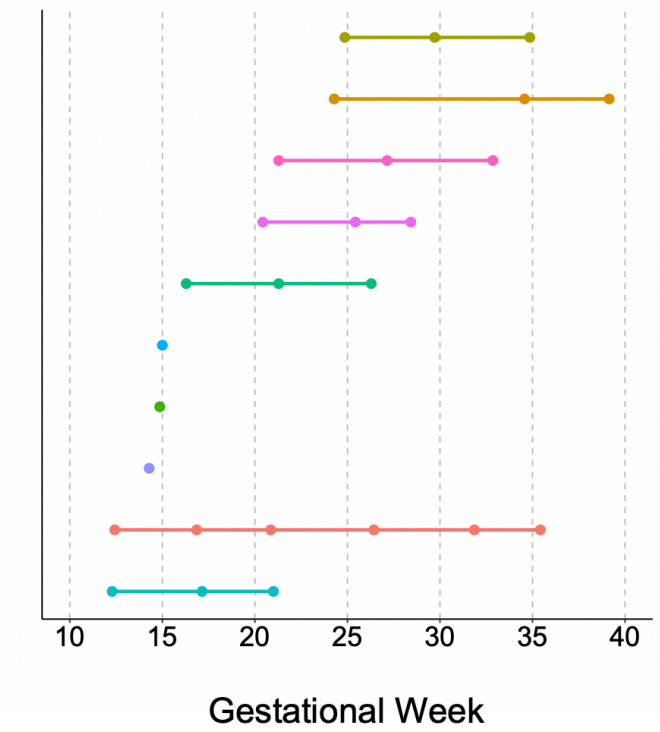

Fig. 1. Illustration of the gestational weeks range captured for participants.

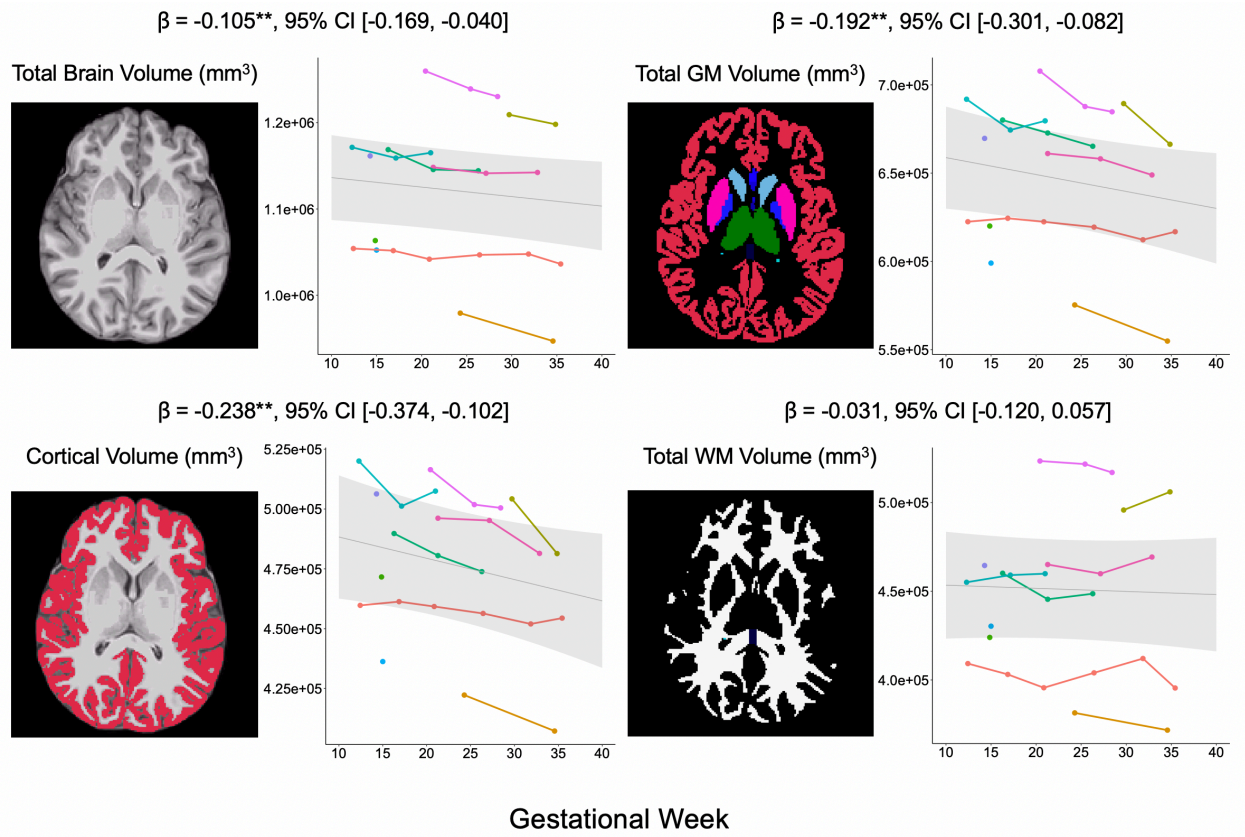

Fig. 2. The observed decrease in brain volumes throughout the course of pregnancy.

Note. ** $p < .01$.

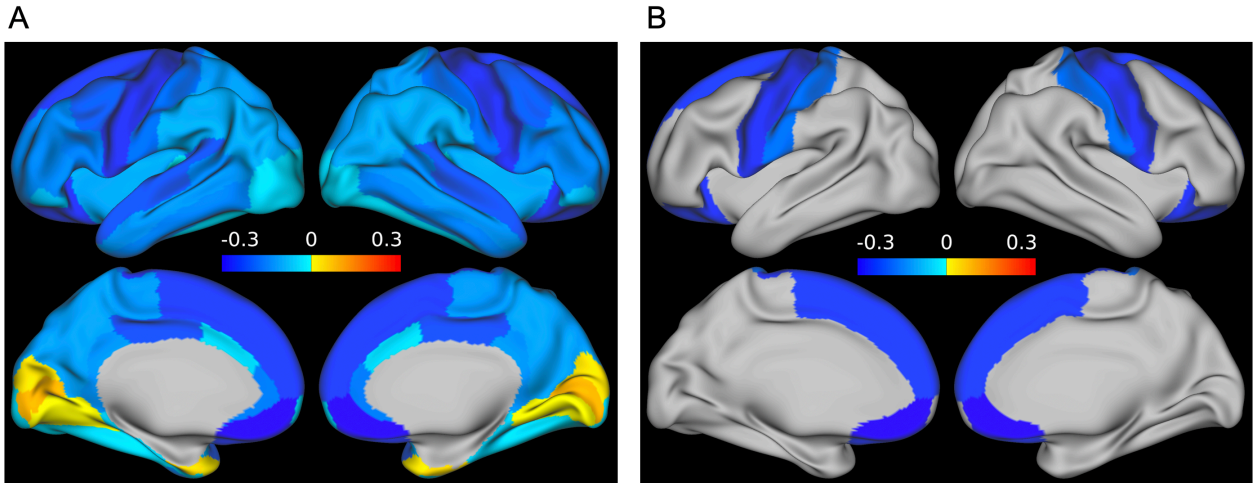

Fig. 3. Illustration of the association between cortical region volumes, as defined by the Desikan-Killiany atlas, and gestational week. A: color-coded to reflect the standardized regression coefficients derived from Linear Mixed Effects models, which were fitted for each cortical region volume against gestational week. B: selectively presents the cortical regions that exhibited a significant volume decrease throughout pregnancy.

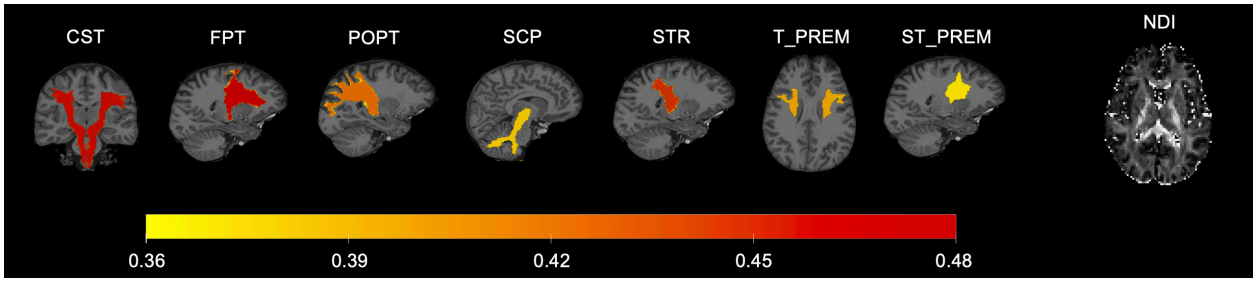

Fig. 4. Illustration of the association between intracellular volume fraction (NDI) and the progression of pregnancy. It was color-coded to represent the standardized regression coefficients from Linear Mixed Effects models fitted for NDI against gestational week.

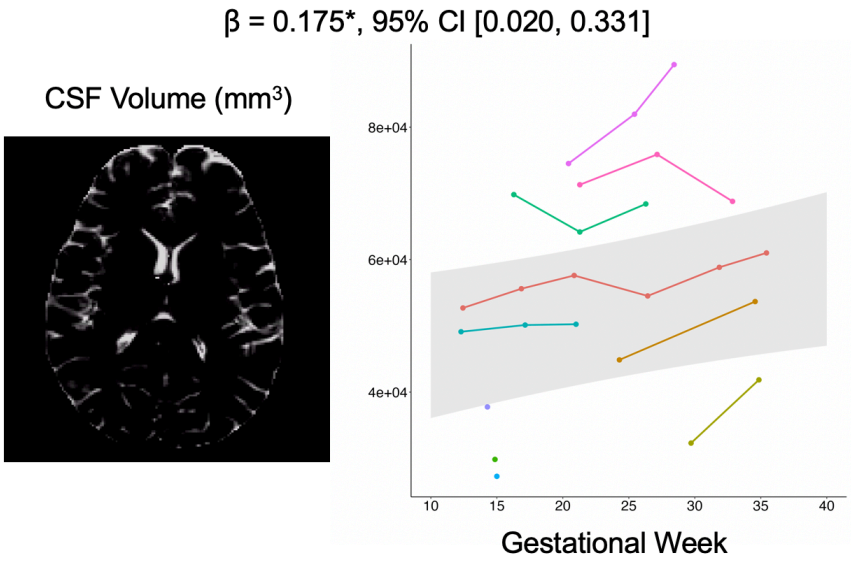

Fig. 5. The increase in total intracranial cerebrospinal fluid (CSF) was observed across pregnancy.

Note. * $p < .05$.

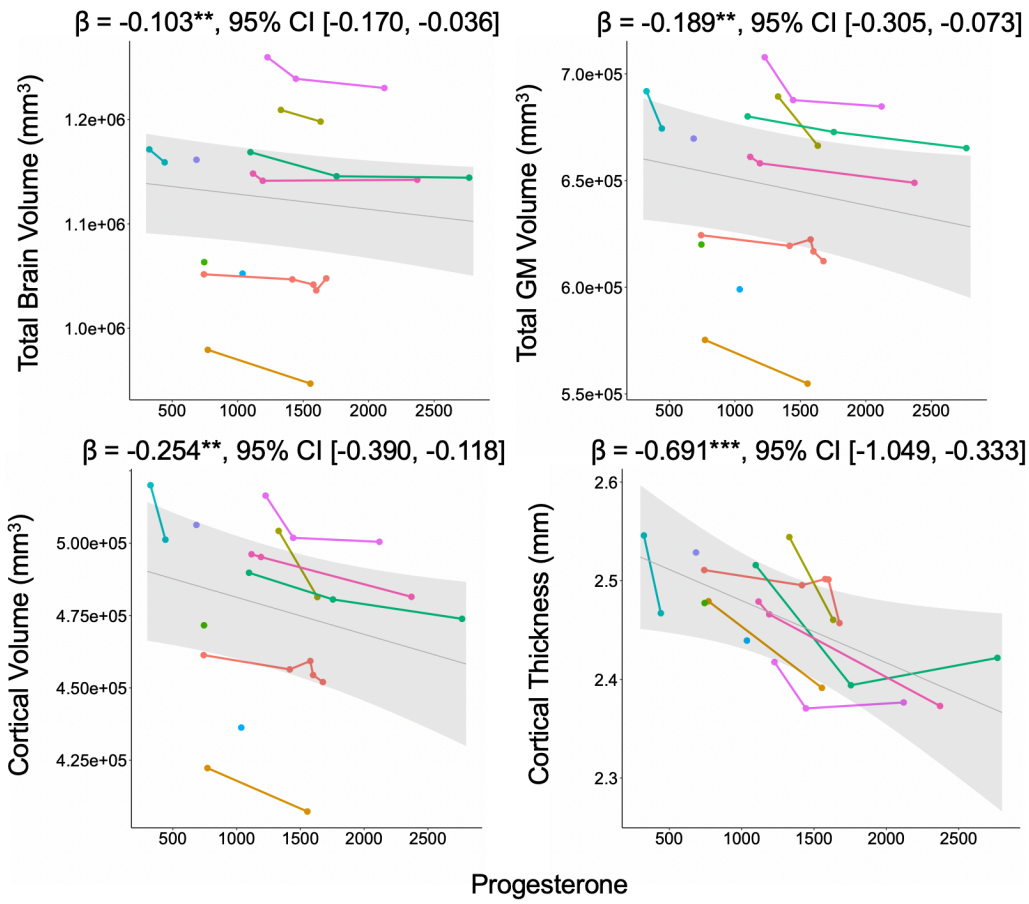

Fig. 6. The observed associations between progesterone levels and brain structural metrics, including total brain volume, total gray matter volume, total cortical volume, and cortical thickness.

Note. ** $p < .01$. *** $p < .001$.

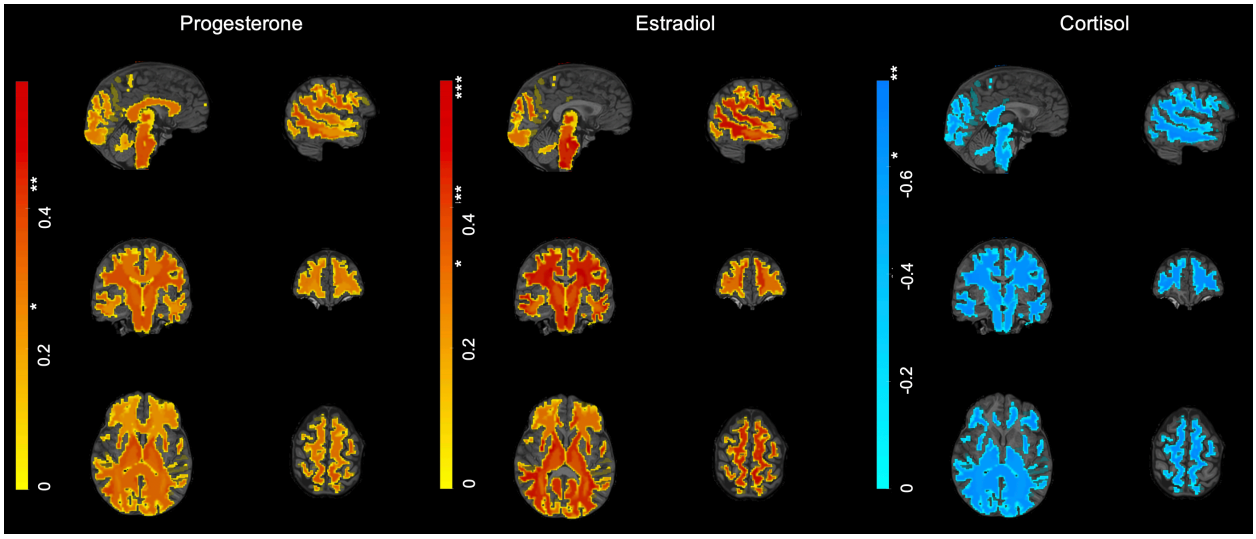

Fig. 7. The association between the intracellular volume fraction (NDI) and hormone levels (specifically progesterone, estradiol, and cortisol). The color-coding reflects the standardized regression coefficients obtained from Linear Mixed Effects models, which were used to analyze the relation between NDI and each of the three hormones.

Note. * $p < .05$. ** $p < .01$. *** $p < .001$. An asterisk in the color bar indicates the level of significance for standardized regression coefficients.